ELSEVIER   0143–8166(95)00013–5

A Hybrid Neural Network for Image Classification

K. Y. Hsu & S. H. Lin

Institute of Electro-Optical Engineering, National Chiao Tung University,
Hsinchu, Taiwan, R.O.C.

&

T. C. Hsieh

Department of Electro-Physics, National Chiao Tung University, Hsinchu,
Taiwan, R.O.C.

ABSTRACT

Principles of the photorefractive perceptron learning algorithm are described. The influences of the finite response time and hologram erasure of the photorefractive gratings on the convergence property of the photorefractive perceptron learning are discussed. A novel neural network which could resolve these constraints is presented. It is a hybrid system which utilizes the photorefractive holographic gratings to implement the inner product between the input image and the interconnection matrix. A personal computer is used for storing the interconnection matrix and the updating procedure, and it also functions as a feedback means during the learning phase. After training the weight vectors are recorded in the volume hologram of an optical processor. This novel method combines the advantages of the massive parallelism of optical systems and the programmability of electronic computers. Experimental results of image classification are presented. It shows that the system could correctly classify the input patterns into one of the two groups after training on four examples in each group during successive iterations. The system has been extended to perform multi-category image classification.

1 INTRODUCTION

In recent years neural networks have been extensively studied.[1,2] The motivation of this research is stimulated by the interest to look for a computing architecture which shares some characteristics of the biological system such that it could address problems such as pattern

recognition that animals do well but current computers do not. The most interesting property of neural networks is the capability of learning. During the learning stage, the network is exposed to a proper set of training samples with an appropriate training algorithm. The networks then adjust their interconnections until each input produces the desired response. After the training is complete the network could be used for information processing such as pattern classification, associative memory and speech recognition. Several types of neural networks have been proposed and demonstrated successfully.[3-5]

On the other hand, optics has been considered as one of the technologies for the implementation of neural networks because the parallel nature of optical systems matches well with that of the neural network. Furthermore, recent progress in photorefractive holography provides a very promising technique for realizing the dynamic interconnections in the neural network. Several optical systems have been proposed and demonstrated.[6-10] In these systems, the learning behavior of the neural network is simulated by updating the holographic dynamic gratings stored in the photorefractive crystal, which responds in real time to the input light intensity distribution. Several problems are encountered in the implementation of photorefractive perceptron networks. First, the dynamic characteristics of the photorefractive grating imply that the stored interconnections are, in addition to being updated by the particular patterns, subject to erasure problems during the training cycles. This results in a restriction to the period of exposure time in the learning process. The mathematical derivation of conditional convergence of this type of neural network was discussed previously.[11,12] It was shown that the sufficient condition for the learning iteration to converge is that the exposure time in each learning iteration be much less than the time constant of the photorefractive crystal. Otherwise, the learning may not converge to a solution. Furthermore, after the training the interconnection weights of the network, which are stored in the photorefractive crystal, will decay during the read-out illumination. Finally, the photorefractive hologram will be erased completely. Therefore, it is difficult to use the same crystal volume for training for the recognition of a new category of images. In other words, the system is difficult to extent to a multi-class case.

In this paper, we present a hybrid method for implementing the perceptron algorithm. It can combine the merits of parallelism of optics and the programmability and non-volatile memory of electronics. In the training stage, the optical part performs the inner product operation of the perceptron. The learning algorithm and the interconnection weights are stored in a personal computer. The influences of the finite response

time and hologram erasure problems on learning behavior in the pure photorefractive network can be avoided. Furthermore, the interconnection is easy to copy and can be used for post-processing. After training, the final weights are transformed into a volume holographic memory in the photorefractive crystal by the angular multiplexing technique. This holographic memory can then be used for optical image classification. In Section 2, principles of the photorefractive optical perceptron are first reviewed. The problem of hologram erasure and its effect on the convergence property of the network are addressed. In Section 3, the hybrid system is presented. The inner product is performed optically using a thin photorefractive crystal plate. On the other hand, the learning algorithm and the interconnection weights are stored in a personal computer. The technique of using a liquid crystal television (LCTV) for performing the bipolar inner product is described. In Section 4, experimental results on using the system for real-time two-category pattern classification are presented. Extension of the system for multi-class image classification is also described. Finally, in Section 5, conclusions are presented.

2 THE PHOTOREFRACTIVE NEURAL NETWORK

In this paper we consider a single layer perceptron network.[13] The network consists of N-input units, an N-dimensional interconnection weight vector $\mathbf{w}$ and one output neuron. Typically, the network is trained to classify a set of training patterns $\{\mathbf{x}_1, \mathbf{x}_2, \ldots, \mathbf{x}_M\}$ into two classes C1 and C2, depending on whether the value of the inner product $|\mathbf{w} . \mathbf{x}_n|$ is greater or smaller than the threshold value θ. During the learning stage, the network is trained according to the learning algorithm to find an appropriate $\mathbf{w}$ for the desired classification.

Several types of photorefractive (PR) neural networks have been proposed and demonstrated for the implementation of the perceptron learning algorithm. In these systems the interconnection weights are recorded as holographic gratings stored in PR crystals such as $LiNbO_3$ and $BaTiO_3$. The PR crystals respond in real-time to the input light intensity distribution, with response time in the range of several tens of milliseconds to a few minutes under an illumination intensity approximately in the range of Watts per cm^2. This finite response property provides the capability for updating the interconnection weights during the learning iterations. The quantity of the weight change for each step can be expressed as $\alpha(p)[1 - e^{-t/\tau}]\mathbf{x}(p)$, where τ is the writing time constant of the crystal, t is the exposure time for each pattern, $\alpha(p)$ is

the updating or error signal and $\mathbf{x}(p)$ is the input pattern at the pth iteration. Since all the holographic gratings are stored in the same volume of the photorefractive crystal, the previously recorded gratings are also illuminated and decayed when an exposure is made to either add or subtract weights to the crystal. Thus, the updating rule of the photorefractive perceptron can be described by the following expression:

$$\mathbf{w}(p+1) = \mathbf{w}(p)e^{-|\alpha(p)|t/\tau} + \sigma(p)[1 - e^{-t/\tau}]\mathbf{x}(p), \tag{1}$$

where $\mathbf{w}(p)$ is the interconnection weight vector at the pth iteration and the updating signal $\alpha(p)$ is expressed by:

$$\alpha(p) = \begin{cases} \quad 0 & \text{if } \mathbf{x}(p) \text{ is correctly classified} \\ \quad 1 & \text{if } \mathbf{x}(p) \in \text{C1, but } |\mathbf{w}(p).\mathbf{x}(p)| < \theta \\ -1 & \text{if } \mathbf{x}(p) \in \text{C2, but } |\mathbf{w}(p).\mathbf{x}(p)| > \theta \end{cases} \tag{2}$$

Note that, in general, the decay time constant for erasing photorefractive holograms and the writing time constant for recording the holograms may be different. The convergence behavior of this case has been shown in Ref. 12. The crystal that we used for the training experiments was $BaTiO_3$, of which the writing and decay time constants are almost equal. Hence, for a simpler illustration, the two time constants are assumed to be equal in eqn (1). Also note that, in the above expression, the absolute value of the inner product is utilized for comparison with the threshold. This is because the photodetectors detect the intensity rather than the amplitude of the light beam. The result is that the threshold value θ for the classification can only be chosen to be positive. Thus, a proper selection of θ is crucial for the learning procedure. If the value of θ is set too low then the patterns in the C2 class will be easily misclassified as class C1, and if θ is chosen too high then it is difficult to obtain a correct $\mathbf{w}$ for classifying the C1 patterns. In either case, the learning will take a large number of iterations to converge or will never converge.

We present the result of computer simulation. The eight patterns shown in Fig. 1 are used as the training set. The four roman letters $\{\mathbf{A}, \mathbf{C}, \mathbf{S}, \mathbf{V}\}$ are specified as class C1 and the four Arabic numbers $\{\mathbf{2}, \mathbf{3}, \mathbf{4}, \mathbf{5}\}$ are specified as class C2. The sampling grid of each pattern for the computer simulation is 32×32 pixels. The patterns are presented one by one into the system and the value of the inner product $|\mathbf{w}.\mathbf{x}|$ is compared with θ. If the classification is correct then the next pattern is presented; if it is misclassified then the interconnection weight is updated using eqn (1). Each update is called an iteration. The check
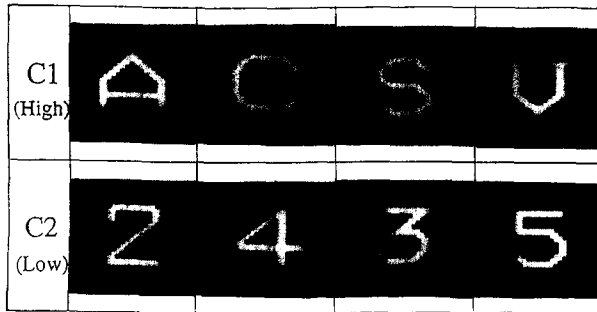
Fig. 1. The training system.

of the eight training patterns is called one cycle. The network is said to be converged when all the eight patterns are correctly classified in a single cycle. The simulation results are shown as the curve with open circles in Fig. 2. The figure shows the number of training cycles for the photorefractive perceptron as functions of the normalized threshold value θ, where θ is normalized, without loss of generality, with respect to the inner product of the character $|\mathbf{A} \cdot \mathbf{A}|$. It is seen that the network converges within six training cycles when θ is chosen between 0·04 and 0·25. On the other hand, the number of training cycles increases rapidly when θ is outside this range. Specifically, if θ is smaller than 0·03 or larger than 0·27 then the error rate remains 100% for all training cycles
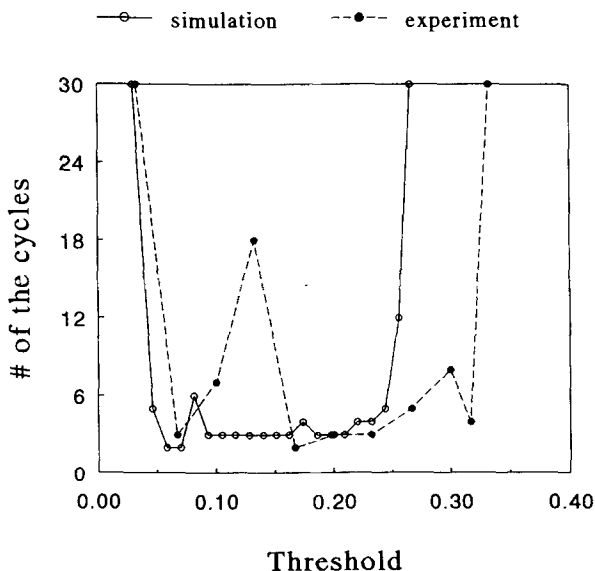

Fig. 2. The number of training cycles as functions of the normalized threshold values. Open circle curve: computer simulations. Filled circle curve: optical experiments.
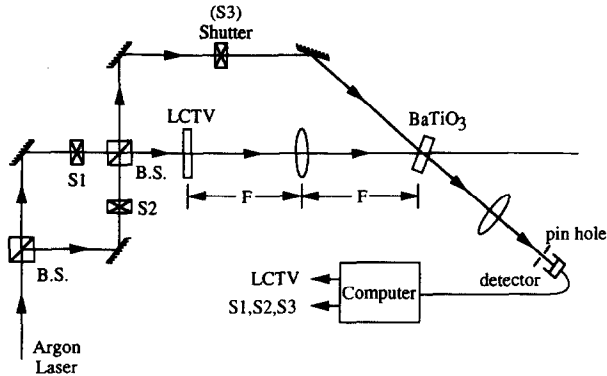
Fig. 3. Optical system for the implementation of the photorefractive perceptron.

and the system does not converge. This is in agreement with our prediction in the previous paragraph that the threshold value must be selected in a proper region for the unipolar photodetectors.

An optical system that was designed to implement the learning algorithm of eqn (1) is shown in Fig. 3. The detailed principle and experimental demonstration of this system have been described in Refs 10 and 13. The system utilizes a photorefractive $BaTiO_3$ crystal for recording the holographic interconnection weight vectors. Shutters S1, S2 and S3 and two beam-splitters form a double Mach–Zehnder interferometer for realizing the addition and erasure of the holographic gratings by using the Stoke theorem for wave reflection and transmission. This interferometer provides a phase control of either 0 (with shutters S1, S3 opened and S2 closed) or π (with shutters S2, S3 opened and S1 closed) phase-shift relative to the initial reference interference fringes. For example, if 0-phase was chosen as the reference, then subtraction of the interconnection strength in the $BaTiO_3$ crystal can be achieved by using the π-phase setting in the subsequent exposures, and addition can be achieved by using the original phase setting (0-phase). By combining these two operations, the learning algorithm of the photorefractive perceptron has been implemented. In our optical experiment, the patterns shown in Fig. 1 are used as the training set. In the training phase, each of the training patterns is sent one by one by the computer to the LCTV as the input to the perceptron. The magnitude of the inner product of the input pattern and the interconnection weights is detected by the photodetector and then compared with the desired value which is stored in the personal computer. The error signal is generated and sent by the computer to turn on the appropriate shutters (S3 and S1 or S2) for updating the weights. The

learning procedure continues until all the patterns are correctly classified. Experimental results are shown as the curve with filled circles in Fig. 2. It is seen that the number of cycles leading to convergence in the optical experiment match well with that of the simulation results, which again confirms our discussion on the restriction of the threshold value.

Next, we discuss the effect of the learning time in each iteration on the convergence of the photorefractive learning network. It is interesting to see from eqn (1) that the existing interconnection weight of $w(k)$ is reduced by a hologram decay factor $\exp(-t/\tau)$ because of the illumination during each of the weight changes. It is clear that the exposure time t plays an important role in determining the magnitude of the incremental weight change, which is in proportion to $[1 - \exp(-t/\tau)]$, as well as the weight decay factor. The derivation for the conditional convergence of photorefractive perceptron learning was given in Refs 11 and 12. Briefly, the perceptron learning will converge provided that the exposure time t is short relative to the time constant τ of the crystal. When the exposure time is too long, then the photorefractive perceptron learning algorithm may not converge to a solution. We have to note that the network discussed in this paper is with a unipolar photodetector which detects the intensity of the output, whereas the results derived in Refs 11 and 12 are based on the learning algorithm that the photodetectors are bipolar and measure the amplitude of the inner products. In the long exposure time region, both networks have the same characteristics for either unipolar or bipolar detections, because in this region the holograms of $w(k)$ decay completely and there is no memory for learning. In the short time region, however, the convergences of the two networks are different.[14] In the bipolar case discussed in Refs 11 and 12, the network can converge for small intervals of exposure, e.g. $t/\tau = 0.0005$ for $\theta = 0$. On the other hand, for the unipolar case described in eqn (1), the network cannot converge if the exposure time is too short. The curve with open circles in Fig. 4 represents the results of computer simulation. The training patterns shown in Fig. 1 are used in this simulation. In Fig. 4 the number of training cycles leading to convergence is shown as a function of the normalized exposure time t/τ. It is seen that when t/τ is smaller than 0.05 the number of training cycles increases rapidly and finally the network may not converge. Optical experiments using the system of Fig. 3 are performed and the results are shown as the curve with filled circles in Fig. 4. The experimental results are in good agreement with the computer simulations.

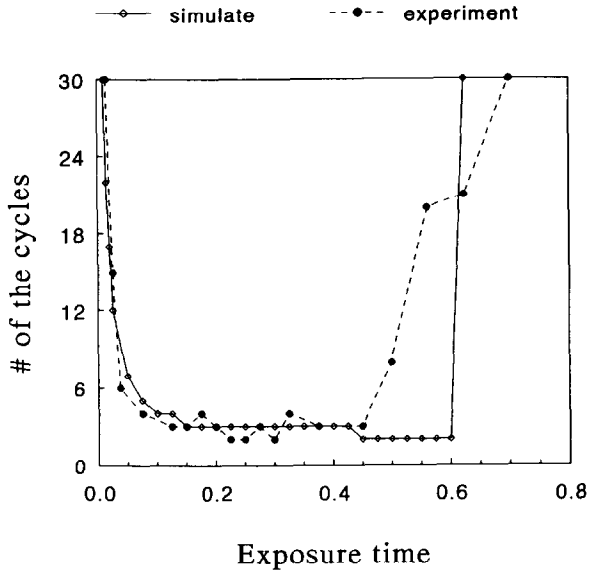The previous discussion shows that there are two factors that affect

Fig. 4. The number of training cycles as functions of the normalized exposure time. Open circle curve: computer simulations. Filled circle curve: optical experiments.

the convergence behavior of the unipolar photorefractive perceptrons: the photodetector threshold value θ and the normalized exposure time t/τ. Only an appropriate selection of these factors can lead to convergence. One possible way to avoid the influence imposed by the exposure time is using an algorithm with a learning rule which does not depend on the updating time t. Furthermore, in order to release the constraint by the threshold value, bipolar signals should be used for comparing with the threshold value.[14] Conventional perceptron learning provides these properties. In the next section we describe a hybrid method for the implementation of the conventional perceptron algorithm.
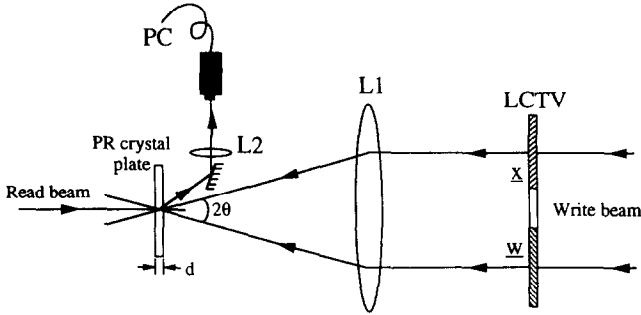
3 THE ARCHITECTURE OF THE HYBRID PERCEPTRON

The algorithm of conventional perceptron learning can be written as[15]

$$w(p + 1) = w(p) + \alpha(p)x(p), \qquad (3)$$

where

$$\alpha(p) = \begin{cases} 0 & \text{if } x(p) \text{ is correctly classified} \\ 1 & \text{if } x(p) \in C1, \text{ but } w(p) \cdot x(p) < \theta \\ -1 & \text{if } x(p) \in C2, \text{ but } w(p) \cdot x(p) > \theta \end{cases} \qquad (4)$$

Fig. 5. The joint transform correlation structure for performing the optical inner product.

Three operations have to be performed for the implementation of this algorithm: (1) updating rule; (2) memorizing the interconnection weights **w**; (3) inner product operation **w.x** and the thresholding. In our system the first two operations are achieved using a personal computer and the third operation is performed by an optical system. This hybrid system removes the constraints on learning by the hologram erasure problem and the finite response time of the photorefractive perceptron. In addition, it combines the advantages of parallelism of optical computing and the programmability of electronic computers.

We now describe how to implement the optical inner product using thin photorefractive crystal plates. The architecture is based on the joint transform correlator.[16] Figure 5 shows the schematic diagram. In operation the two patterns $\mathbf{w}(p)$ and $\mathbf{x}(p)$ are presented simultaneously onto the LCTV. Each pattern occupies half the screen of the LCTV and they are Fourier transformed by lens L1. A thin photorefractive plate, which is an iron-doped LiNbO$_3$ plate in our case, is put at the Fourier plane of L1. The interference fringes of the Fourier spectra $\mathbf{W}(p)$ and $\mathbf{X}(p)$ induce phase gratings in the photorefractive plate. The gratings are read out by a read beam incident from the back side of the crystal. In our experiments, the incidence angle $2\theta = 4^0$, $d = 49$ μm. Therefore, the hologram parameter $Q < 1$, and the Raman–Nath diffraction condition for the thin hologram is satisfied. Under this condition, the first order diffraction amplitude of the read beam can be expressed as[17]

$$E_{d1} \approx J_1\left(\frac{\omega}{c}\frac{n_1 d}{\cos \theta}\right),$$
(5)

where J_1 is the Bessel function of the first kind, c is the speed of light, ω is the light frequency and n_1 is the photorefractive index change of the LiNbO$_3$ plate. Normally, n_1 is less than 10^{-4}; thus $\omega n_1 d/c \cos \theta \ll 1$ and

the above Bessel function can be approximated by its argument in parentheses, i.e.

$$J_1\left(\frac{\omega \ n_1 d}{c \cos \theta}\right) \approx \frac{\omega \ n_1 d}{c \cos \theta}. \qquad (6)$$

Furthermore, since n_1 is proportional to the interference fringes, **WX* + W*X**, thus, by combining these equations, the first order diffraction is expressed by

$$E_{d1} \sim \mathbf{WX}^* + \mathbf{W}^*\mathbf{X}. \qquad (7)$$

Finally, E_{d1} is Fourier transformed by lens L2 and the output signal is detected at the center of the Fourier plane. The detected signal can be written as

$$\text{output signal} \sim |\mathscr{T}\{E_{d1}\}|_{x=0, y=0}|$$
$$\sim |\mathscr{T}\{\mathbf{W}^*\mathbf{X}\}|_{x=0, y=0}|$$
$$\sim |\mathbf{w} \cdot \mathbf{x}|, \qquad (8)$$

where $\mathscr{T}$ represents the Fourier transformation. Therefore, the inner product $|\mathbf{w} \cdot \mathbf{x}|$ is obtained.

In this paper we consider the case where **x** are patterns with positive value elements (0–255 grey levels), whereas **w** can be bipolar because it is the result of addition and subtraction of the patterns **x**. Thus, we need a bipolar spatial light modulator for displaying the bipolar weighted patterns. In our experiments, the LCTV is operated in amplitude modulation mode, which has only unipolar grey levels from zero to 255. To resolve this problem, the bipolar **w** is expressed as the summation of two positive unipolar vectors:

$$\mathbf{w} = \mathbf{w}^+ - \mathbf{w}^-, \qquad (9)$$

where $\mathbf{w}^+$ is the vector whose positive elements are equal to the corresponding positive elements of **w**, with the other elements of $\mathbf{w}^+$ set to zero, which corresponds to zero and negative elements of **w**. In a similar way, $\mathbf{w}^-$ corresponds to the non-positive part of **w**. In the experiment, there are two steps for each inner product operation. In the first step, $\mathbf{w}^+$ and **x** are presented on the LCTV and $\mathbf{w}^+ \cdot \mathbf{x}$ is detected by the optical detector. In the second step, $\mathbf{w}^-$ and **x** are displayed and $\mathbf{w}^- \cdot \mathbf{x}$ is detected. Then the two signals are subtracted in the personal computer. Since

$$\mathbf{w}^+ \cdot \mathbf{x} - \mathbf{w}^- \cdot \mathbf{x} = (\mathbf{w}^+ - \mathbf{w}^-) \cdot \mathbf{x}$$
$$= \mathbf{w} \cdot \mathbf{x}, \qquad (10)$$

the inner product $\mathbf{w} \cdot \mathbf{x}$ is obtained. Thus, $\mathbf{w} \cdot \mathbf{x}$ is bipolar and the threshold value θ can also be selected as zero or in bipolar values.
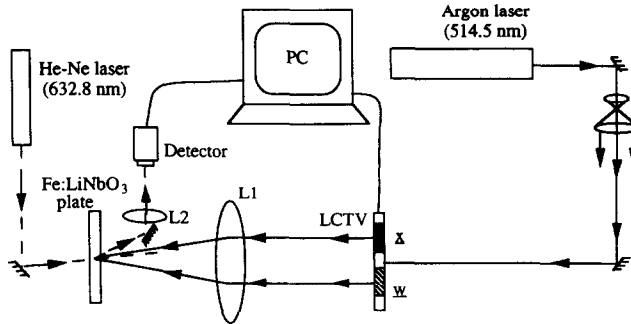
Fig. 6. The set-up for the implementation of hybrid perceptron learning.

4 EXPERIMENTAL RESULTS

The hybrid system shown in Fig. 6 was assembled to implement the conventional perceptron learning. In the system, a collimated argon laser beam at 514·5 nm wavelength is used for writing the joint transform hologram of the input pattern **x** and the interconnection weight vector **w**. The holograms are recorded in the thin photorefractive LiNbO$_3$ plate. A He–Ne laser is used for reading the holographic gratings. The readout signal is Fourier transformed by lens L2 to obtain the inner product. This product is detected by the photodetector and sent to the personal computer for the learning control. In the experiment, the initial values of **w** are set to zero, and the patterns in Fig. 1 were used as the training samples **x**, of which {**A, C, S, V**} were specified as class C1 and {**2, 3, 4, 5**} were specified as class C2. The threshold value was arbitrarily set to zero. Figure 7 shows the training
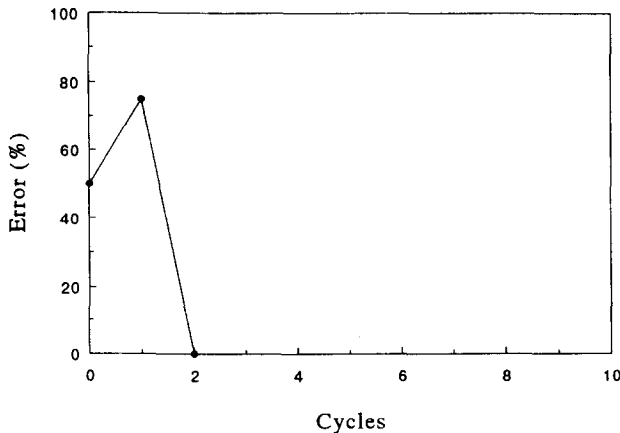

Fig. 7. The learning curve of hybrid perceptron learning.

curve. It is seen that the patterns are correctly classified after two cycles of training. After the training is complete, the desired interconnection weight vectors $\mathbf{w}^+$ and $\mathbf{w}^-$ are obtained and stored in the personal computer. The weight interconnections $\mathbf{w}^+$ and $\mathbf{w}^-$ are non-volatile and the system is ready for pattern classification application.

Note that, in principle, we can use the joint transform correlator to perform the inner product operations in the calculation of $\mathbf{w} \cdot \mathbf{y}$ for image classification. However, this calculation needs three steps: $\mathbf{w}^+ \cdot \mathbf{y}$, $\mathbf{w}^- \cdot \mathbf{y}$ and the subtraction $(\mathbf{w}^+ \cdot \mathbf{y} - \mathbf{w}^- \cdot \mathbf{y})$. In order to make further use of the parallelism of optical systems for information processing, $\mathbf{w}^+$ and $\mathbf{w}^-$ are transformed into holographic memories in one crystal volume by using a multiplexing technique. By doing this, we obtain an optical processor which performs two-channel inner products, $\mathbf{w}^+ \cdot \mathbf{y}$ and $\mathbf{w}^- \cdot \mathbf{y}$, in parallel. The subtraction of $\mathbf{w}^+ \cdot \mathbf{y}$ and $\mathbf{w}^- \cdot \mathbf{y}$ is obtained electronically. Thus, the inner product $\mathbf{w} \cdot \mathbf{y}$ can be achieved in one step. There are several techniques for recording multiple holograms in a crystal volume, such as angular, wavelength and phase multiplexing techniques.[18–22] In our experiment, we chose angular multiplexing. Figure 8 shows the schematic diagram of the complete system; an optical processor is added into the learning system. In the figure, the parts outside the dashed block form the learning network, whereas rotated mirror M1, lenses L3, L4, L5, photorefractive crystal Fe:LiNbO$_3$ and the detector pair form the optical processor. This processor is, in fact, the structure of a correlation system. For recording the memories of $\mathbf{w}^+$ and $\mathbf{w}^-$, first $\mathbf{w}^+$ is presented at the position of $\mathbf{w}$
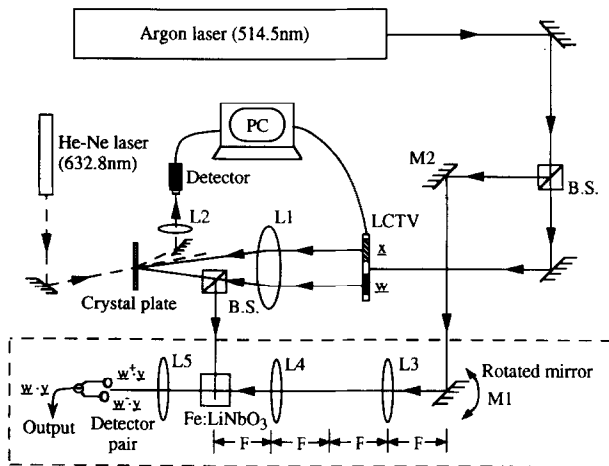
Fig. 8. The complete set-up for the hybrid perceptron and the optical processor. PC, personal computer.

on the LCTV. The Fourier transform hologram of w^+ is recorded on the $Fe:LiNbO_3$ crystal. A plane wave as the reference beam for this recording is provided by the argon laser through beam-splitter BS, mirror M2 and the telescope structure of M1, L3 and L4. The reference beam intersects with the Fourier spectra W^+ at an angle of 90°. Then, similarly, w^- is displayed at the same position of w on the LCTV and its Fourier transform hologram is recorded in the crystal using the reference beam at a slightly different angle. The multiplexing of the reference beam is provided by rotating M1 of the telescope structure. After the Fourier transform holograms are recorded, the system is ready for the pattern classification operation. The patterns to be classified, for example y, are presented at the position of w on the LCTV. Then, the inner products $w^+ . y$ and $w^- . y$ are obtained simultaneously and are detected by the detector pair. Subtraction of the two detected values provides the final output. Table 1 shows the results of the experiments. The first column shows the input pattern. Corresponding to each input there are two optical signals, $w^+ . y$ and $w^- . y$, the values of which are shown in the second and third columns. Then, the inner product $w . x$ is obtained and is shown in the fourth column. Finally, according to whether the inner is higher or lower than the threshold value, the fifth column shows the classification of each pattern. It is seen from the table that the patterns are correctly classified.

TABLE 1

Experimental Results of Optical Pattern Classification

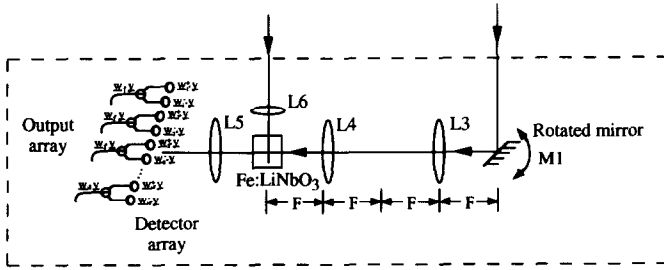| Input pattern	Optical output		$\underline{w} . \underline{x}$	Class
	$\underline{w}^+ . \underline{x}$	$\underline{w}^- . \underline{x}$		
	99	2	97	C1
	190	10	180	C1
	4	36	-32	C2
	21	38	-17	C2

Fig. 9. The optical processor for multi-class image classification.

An additional advantage for using the multiplexing holograms to perform the inner product operation is that the system can easily be extended to the multi-category cases.[23] In order to perform the multi-class inner product operation, we need an optical processor to replace that in the two-category case. To achieve this, the interconnection weight vector for each class is firstly obtained one by one using the hybrid perceptron learning shown in Fig. 6. Each weight vector is stored in the computer. After the training for all the classes is complete, each weight vector is recorded as a Fourier transform hologram in the photorefractive crystal using the angular multiplexing technique. The holograms for the w^+ and w^- pair of each class are recorded at the neighboring angles. Thus, there is an M-pair detector array for the M-class classifier, with the neighboring detectors forming a pair for the detection of $w^+ . y$ and $w^- . y$. In this way, the two-category classification is extended to the M-class case. The schematic diagram of the M-class optical processor is shown in Fig. 9.

In our experiment, a system is assembled for the recognition of 10 handwritten Chinese characters. Therefore, there are 10 pairs of holographic interconnection vectors, 10 for w^+ and the other 10 for w^-. The 20 weight vectors are recorded in the $LiNbO_3$ crystal using the angular multiplexing technique. When an input image is displayed at the position of w on the LCTV, the output of the multi-channel inner product is detected by the linear array of photodetectors. The signal is sent to the computer to produce the array of the recognition signal. The experimental results are shown in Table 2. The first column shows the input images. The second column shows the relative value of the inner product produced by the output array. The third column shows the recognized output. From the upper two rows of the table, it is seen that both the rotated versions of one character produce a high inner product at the first position of the output array. Both are recognized as class C1. Also, from the lower two rows of the table, it is seen that both

TABLE 2
Experimental Results of Multi-class Image Classification

Input pattern	Inner product $\underline{w} \cdot \underline{y}$	Recognized output
		C1
		C1
		C4
		C4

distorted versions of another character produce high values of inner product at the fourth position of the array. They are recognized as class C4. The experimental results show that the system can perform multi-class image classification in parallel, and it has the capability of rotation and distortion invariance.

5 CONCLUSION

We have described the principles of the photorefractive perceptron learning network. The influences of the finite response time and hologram erasure problem on the convergence properties of the photorefractive perceptron are discussed. To overcome these constraints for learning, we have presented and demonstrated a novel system which utilizes thin photorefractive plates for performing optical inner product and a personal computer for the learning control and storage of the interconnection weights. Our system is, in fact, the

implementation of the conventional perceptron algorithm. Therefore, the system can work for both the binary images (with levels 0 and 1) and the grey level images. Also, the storage capacity, or the maximum numbers of patterns that can be classified, is equal to two times the number of the input neurons. After the learning is complete, the interconnection weights are transformed into holographic memories using the angular multiplexing technique. The system has been extended to a multi-channel case to perform parallel processing of multi-category image classification. Experimental results of using the optical system for pattern classification are presented. The system combines the advantages of the learning capability of the perceptron network and the parallel processing of information of optical systems.

ACKNOWLEDGEMENT

REFERENCES

1. Rumelhart, D. E. & McClelland, J. M. (Eds), *Parallel Distributed Processing*, Vols I and II. MIT Press, Cambridge, MA, 1986.
2. Denker, J. S. (Ed.), *Neural Networks for Computing*, AIP Conference Proceedings, Vol. 151. American Institute of Physics, New York, 1986.
3. Hopfield, J. J., Neural networks and physical systems with emergent collective computational abilities. *Proc. Natl. Acad. Sci. U.S.A.*, **79** (1982), 2554–2558.
4. Hopfield, J. J., Neurons with graded response have collective computational properties like those of two-state neurons. *Proc. Natl. Acad. Sci. U.S.A.*, **81** (1984), 3088–3092.
5. Hsu, K. Y., Li, H. Y. & Psaltis, D., Optical implementation of a fully connected neural network. *Proc. IEEE*, **78** (1990), 1637–1645.
6. Abu-Mostafa, Y. S. & Psaltis, D., Optical neural computers. *Scient. Am.*, **256** (1987), 88–94.
7. Psaltis, D., Brady, D. & Wagner, K., Adaptive optical networks using photorefractive crystals. *Appl. Opt.*, **27** (1988), 1752–1759.
8. Hsu, K., Brady, D. & Psaltis, D., Experimental demonstration of optical neural computers. *Proc. on Neural Information Processing Systems*, pp. 377–386. American Institute of Physics, New York, 1988.
9. Paek, E. G., Wullert, J. & Patel, J. S., Holographic implementation of a learning-machine based on a multicategory perceptron algorithm. *Opt. Lett.*, **14** (1989), 1303–1305.

10. Hong, J., Campbell, S. & Yeh, P., Optical pattern classifier with perceptron learning. *Appl. Opt.,* **29** (1990), 3019–3025.
11. Hsu, K. Y., Lin, S. H. & Yeh, P., Conditional convergence of photorefractive perceptron learning. *Opt. Lett.,* **18** (1993), 2135–2137.
12. Cheng, C. J., Yeh, P. & Hsu, K. Y., Generalized perceptron learning rule and its implications for photorefractive neural networks. *J. Opt. Soc. Am. B.,* **11** (1994), No. 9.
13. Hsu, K. Y., Lin, S. H., Cheng, C. J., Hsieh, T. C. & Yeh, P., An optical neural network for pattern recognition. *Int. J. Opt. Comput.,* **2** (1991), 409–423.
14. Cheng, C. J., Hsu, K., Lin, S. H., Hsieh, T. C. & Yeh, P., An optical learning network with amplitude detection. *Proc. SPIE,* **1806** (1992), 488–499.
15. Rosenblatt, F., *Principles of Neurodynamics: Perceptron and the Theory of Brain Mechanisms,* p. 97. Spartan Books, Washington, DC, 1962.
16. Yu, F. T. S. & Lu, X. J., A real-time programmable joint transform correlator. *Opt. Commun.,* **52** (1984), 10–16.
17. Yariv, A. & Yeh, P., *Optical Waves in Crystals,* p. 358. Wiley Interscience, New York, 1983.
18. Chen, F. S., laMacchia, J. T. & Fraser, D. B., Holographic storage in lithium niobate. *Appl. Phys. Lett.,* **13,** No. 7 (1968), 223–225.
19. Mok, F. H., Tackitt, M. C. & Stoll, H. M., Storage of 500 high resolution holograms in a LiNbO₃ crystal. *Opt. Lett.,* **16** (1991), 605–607.
20. Mok, F. H., Angle-multiplexed storage of 5000 holograms in lithium niobate. *Opt. Lett.,* **18** (1993), 915–917.
21. Rakuljic, G. A., Leyva, V. & Yariv, A., Optical data storage by using orthogonal wavelength-multiplexed volume holograms. *Opt. Lett.,* **17** (1992), 1471–1473.
22. Denz, C., Pauliat, G., Roosen, G. & Tschudi, T., Potentialities and limitations of hologram multiplexing by using the phase-encoding technique. *Appl. Opt.,* **31** (1992), 5700–5705.
23. Hsu, K. Y., Lin, S. H. & Hsieh, T. C., Real-time image processing using photorefractive crystals, Paper 27C1, *Int. Conf. on Optical Memory & Neural Network,* Moscow, 27–30 Aug. 1994.